17th World Conference on Earthquake Engineering, 17WCEE
Sendai, Japan - September 13th to 18th 2020

STRUCTURAL BEHAVIOR OF CFT BEAM-COLUMNS WITH HIGH STRENGTH STEEL SUBJECTED TO CYCLIC LOADING

M. Kido[(1)], D. Fujioka[(2)] and K. Jyozaki[(3)]

[(1)] *Associate Professor, The University of Kitakyushu, kido-m@kitakyu-u.ac.jp*
[(2)] *Graduate student, Graduate school of the University of Kitakyushu, z8mbb024@eng.kitakyu-u.ac.jp*
[(3)] *Graduate student, Graduate school of the University of Kitakyushu, z8mbb012@eng.kitakyu-u.ac.jp*

Abstract

The impacts of the Nankai Trough megathrust earthquake on super high-rise buildings are of significant concern. Concrete filled steel tubular (CFT) columns are typically used in the construction of these buildings and their natural periods are long. Based on this, flexural and shear experimental works of square CFT columns under constant rotation angle have already been reported. These test parameters were the effective length - depth ratio, the axial force ratio, the width-thickness ratio, the strength of the materials and the magnitude of the rotation angle. However, high strength 780N/mm^2 steel for building structure (H-SA700) was not used in these studies. The purpose of this study is to determine the structural behavior of CFT beam-columns using H-SA700 steel under a constant axial load and rotation angle.

The test specimen was a CFT beam-column having a square cross-section and fabricated from H-SA700 high-strength steel. The nominal width-thickness ratio of a steel plate element was 21. The compressive strength of the concrete cylinder was approximately 100N/mm^2. The test specimens were cantilevered columns and were subjected to the constant axial load and a cyclic lateral load. Three specimens were tested using the following test parameters, the axial force ratios n=0.3 and 0.4 and rotation angles R=2% and 2.5%.

The relationship between the lateral force Q and the rotation angle R is shown along with photos taken after the test. Local buckling and cracks occurred in all specimens and the strength of all specimens decreased with each cycles. In the specimens with n=0.3 and R=2.5% and with n=0.4 and R=2%, crack sizes were relatively larger, and the deformation by the local buckling was small. The strength deterioration of these specimens is dominated by the cracks. In constant, in the specimen with n=0.4 and R=2.5%, deformation by local buckling was relatively large, and crack occurred only at the corner of the cross-section. The strength deterioration of this specimen was dominated by the local buckling.

The amounts of strength deterioration Q_i/Q_{max} are shown, where Q_i is the strength at the maximum/minimum rotation angle of the i-th cycle, and $Q_{\max}$ is the maximum strength. Behavior of the test specimen with n=0.4 and R=2.5% was not affected by the crack and the strength deterioration was constant regardless of positive or negative loading. In the test specimens with n=0.3 and R=2.5% and with n=0.4 and R=2% the difference between the positive and negative sides is significantly large because the size of cracks were relatively large.

A limit-repeated cycle number is defined by the number of cycles that the lateral load at the maximum rotation angle decreased by 95%, 90%, 85% and 80% of the maximum lateral load. The relationship between the plasticity ratio and the limit-repeated cycle numbers $N_{95\%}$ and $N_{80\%}$ are shown. The limit-repeated cycle numbers $N_{95\%}$ and $N_{80\%}$ have negative correlation with the plasticity ratio μ. By comparing with the results obtained by previous experimental study using BCR295 steel, we see that the relationship between $N_{95\%}$ and the plasticity ratio μ is almost same. The value of $N_{80\%}$ of this study is smaller than that of the previous study.

We conclude from the experimental study that there are two failure modes which determine the strength deterioration behavior in these beam-columns. One is of a crack-dominant type and the other is of a local buckling-dominant type.

Keywords: Steel concrete composite structure, Long period ground motion, Cyclic behavior, High strength materials

1. Introduction

The impacts of the Nankai Trough megathrust earthquake on super high-rise buildings are of significant concern. Concrete filled steel tubular (CFT) columns are typically used in the construction of these buildings and their natural periods are long. Based on this, flexural and shear experimental works of square CFT columns under constant rotation angle have already been reported [1-5]. These test parameters were the effective length - depth ratio, the axial force ratio, the width-thickness ratio, the strength of the materials and the magnitude of the rotation angle. However, high strength 780N/mm2 steel for building structure (H-SA700) was not used in these studies [6-7]. The purpose of this study is to determine the structural behavior of CFT beam-columns using H-SA700 steel under a constant axial load and rotation angle.

2. Experiment

2.1 General

The test specimen is a concrete filled steel tubular beam-column of which steel portion is a square cross-section. Nominal width-thickness ratio of a steel plate element is 21. The material of steel portion is H-SA700 high-strength steel. The compressive strength of concrete is approximately 100N/mm^2.

Specimens are subjected to alternating horizontal load with constant displacement under constant axial load as shown in Fig.1.

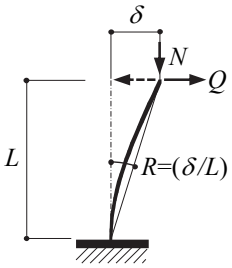

Fig. 1 – Loading condition

2.2 Experimental parameters

As the experimental parameters, displacement δ (rotation angle $R = \delta/L$ of a beam-column, L: length of a member) and axial load ratio n ($=N/N_0$, $N_0 = {}_sA_s\sigma_y + {}_cA_c\sigma_B$, ${}_sA$, ${}_cA$: cross section of steel portion and concrete portion respectively, ${}_s\sigma_y$: yield strength of steeel tube and, ${}_c\sigma_B$: compressive strength of concrete) are selected, and they vary as follows; R=2 and 2.5%, n=0.3 and 0.4. Total three specimens are tested and test conditions of specimens are shown in Table 1. Naming rule of the test specimens is shown below Table 1. In Table 1, ${}_sN_y$ is a yield axial strength of steel tube portion and ${}_cN_0$ is an ultimate strength of concrete portion.

Table 1 Specimen list

No.	Specimen	R (%)	n	${}_c\sigma_B$ (N/mm^2)	N (kN)	${}_sN_y/{}_cN_0$
1	LD12n30R25	2.5	0.3	101	1078	1.88
2	LD12n40R2	2	0.4	99.2	1429	1.91
3	LD12n40R25	2.5	0.4	101	1438	1.88

Naming rule : LD12n30R25 LD12 : l_k/D =12 n30:n =0.3 R25:R =2.5%

2.3 Specimen

Figure 2 (a) shows the shape and size of test specimen. At first, two channel shapes are made by bending a H-SA700 steel plate, and a square shaped column is made by welding two channels as shown in Fig.2 (c). A thickness of the plate is 6mm. Table 2 shows the measured value of the steel tube. In Table 2, R_o and R_i are the outer and inner radius of the corner. The length of the specimen L is 750mm and the effective length factor-depth ratio is 12. The welding condition is as follows;

1) Welding heat input: 10.7kJ/cm (maximum value)

2) Interpass temperature: 125 degrees Celsius (maximum value)

3) Number of layers: 2

4) Welding material: YM-80A.

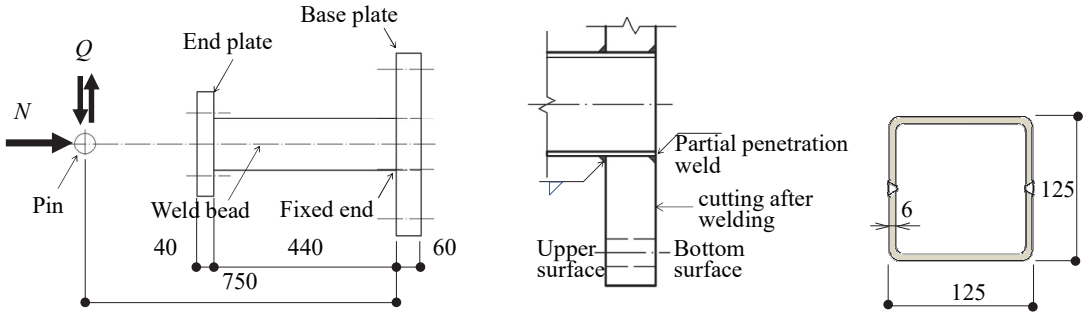

(a) Specimen (b) Welding detail at column base (c) Section

Fig. 2 – Shape of specimen (unit: mm)

Table 2 – Measured dimensions of steel tubes

Depth D (mm)	Width B (mm)	Plate thickness t (mm)	Width-thickness ratio B/t	Section area of steel tube A(mm^2)	Outor radius R_o (mm)	Inner radius R_i (mm)
124.5	127.5	6.417	19.9	2919	16.9	10.5

An end plate is attached to free-end of a specimen by fillet welding. A base plate is attached to the fixed-end of a specimen by following procedure. A square opening which is same shape of the specimen is made in the baseplate and the square pipe is inserted to the opening then the pipe and the baseplate are welded as shown in Fig. 2(b). After welding, the cutting is performed to make a plane surface. The welding condition is as follows:

1) Welding heat input: 6.6kJ/cm

2) Interpass temperature: 121 degrees Celsius

3) Number of layers: 1

4) Welding material: YM-55C

5) preheat temperature: 105 degrees Celsius

2.4 Mechanical Properties

In addition to the tensile test of steel coupon, vacant stub columns of steel tubes, a CFT stub column and concrete cylinders were tested under compression to examine the stress-strain relations. Average yield stresses are equal to 791 N/mm^2 and average ultimate strength equal to 856N/mm^2 both obtained from tensile

test as shown in Table 3. Examples of stress-strain relations of steel plates obtained from the tensile test are shown in Fig. 3 (a).

The concrete mix proportion is shown in Table 4. The average compressive strength ${}_c\sigma_B$ of concrete cylinder was 100N/mm^2. Examples of stress-strain relations of concrete are shown in Fig. 3 (b).

Measured dimensions of the steel tubes for stub columns are shown in Table 5 and results of stub column tests are shown in Table 6. The ultimate strengths of the vacant stub columns and the CFT column are 2530kN (average value) and 3576kN. Load and displacement relations are shown in Fig. 4.

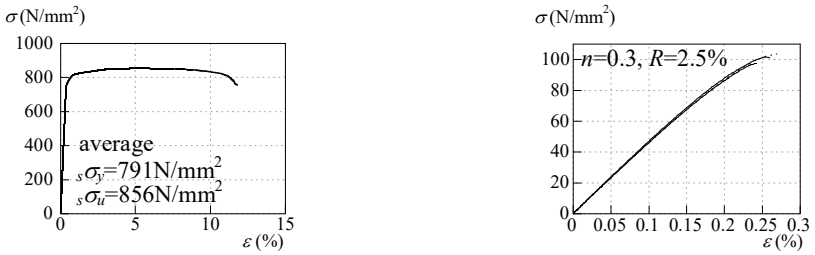

(a) Steel (b) Concrete

Fig. 3 – Stress-strain relations

Table 3 – Mechanical properties of steel tube

Yield sterength ${}_s\sigma_y$(N/mm^2)	Ultimate strength ${}_s\sigma_u$(N/mm^2)	Yield ratio ${}_s\sigma_y/{}_s\sigma_u$	Breaking elongation *EL*	Yield strain ε_y (%)	Young's modulus *E*(N/mm^2)
791	856	92.5%	10.2%	0.384	2.06×10^5

Table 4 – Concrete mix proportion

F_c (N/mm^2)	W/C ratio (%)	Cement (kg/m^3)	Water (kg/m^3)	Fine Aggregate (kg/m^3)	Caorse Aggregate (kg/m^3)	Ad-mixture (kg/m^3)
72	27.0	630	170	740	870	11.66

Table 5 –Stub column specimen list and measured dimensions

Specimtn No.	Vacant tube /CFT	Depth *D* (mm)	Width *B* (mm)	Plate thickness *t* (mm)	Length *L* (mm)	Section area of steel tube *A*(mm^2)	Outor radius R_o (mm)	Inner radius R_i (mm)
No.1	Vacant tube	124.8	127.4	6.45	375.1	2935	16.9	10.45
No.2		124.2	127.6	6.42	375.4	2916		10.48
No.3	CFT	126.0	126.0	6.39	375.1	2905		10.51

Table 6 – Experimental results of stub columns

Specimen No.	Vacant tube /CFT	P_{max} (kN)	${}_sN_y/N_0$ (kN)	$P_{max}/{}_sN_y$ P_{max}/N_0	δ_{Pmax} (mm)
No.1	Vacant tube	2543	2322	1.10	4.70
No.2		2516	2306	1.09	4.36
No.3	CFT	3576	3568	1.00	2.52

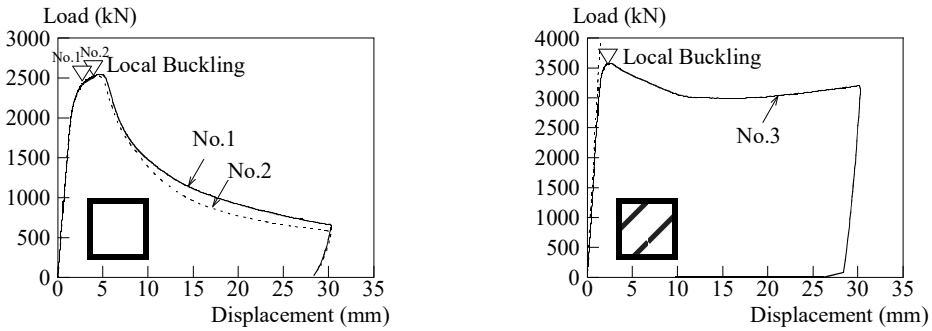

(a) Vacant steel tube (b) CFT

Fig. 4 – Load - displacement relationships of stub columns

2.5 Loading apparatus

Figure 5 shows the experimental apparatus. Constant vertical load N was applied on the specimen by 1500kN hydraulic jack and the horizontal load was applied to the specimen by 500kN hydraulic jack. The amplitude of rotation angle of the column is constant.

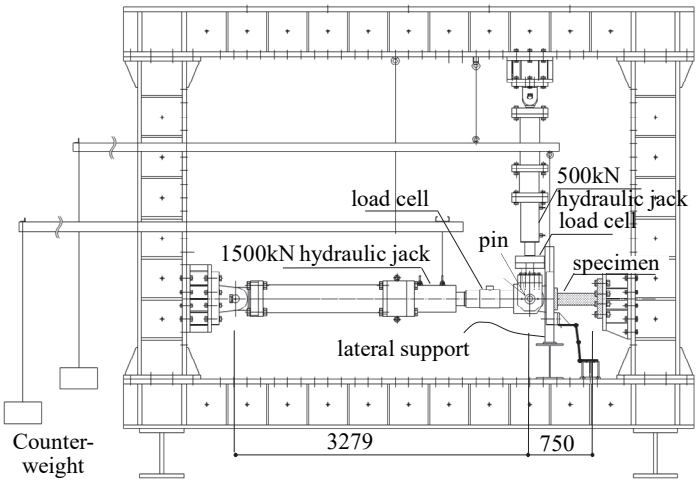

Fig. 5 – Loading apparatus

3. Results and analysis

3.1 Horizontal load -rotation angle relationships

Figure 6 shows the horizontal load (Q) - rotation angle (R) relationships. The experimental behavior is shown by the solid line and the dashed line is the plastic collapse mechanism line obtained by assuming that a plastic hinge is formed at the bottom of the beam-column, and the straight solid line is the elastic line. The numbers in the square is the number of loading cycles. In the figures, mark ◇ indicates the point that the strain measured by a strain gauge reached the yield strain, mark △ shows the maximum lateral load. According to these figure, all specimen strength gradually decreases every cycles. Local buckling and cracks are observed and the cycles when local buckling and crack occurred are shown in Tables 8 and 9 respectively.

Photo 1 shows the test specimens after the experiment. According to these photos, the deformation by local buckling of specimen with n=0.4 and R=2.5% is the largest on the other hand, the deformation by local buckling is hardly noticeable in other specimens.

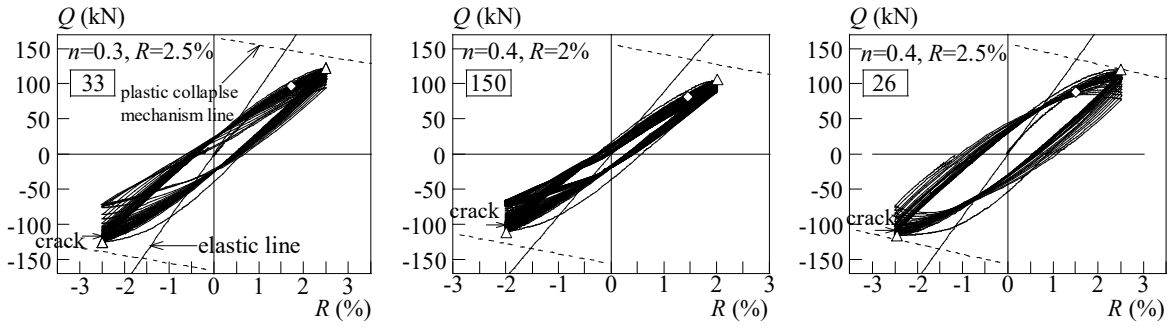

(a) LD12n30R25 (b) LD12n40R2 (c) LD12n40R25

Fig. 6 –Latelal load - rotaion angle relationships

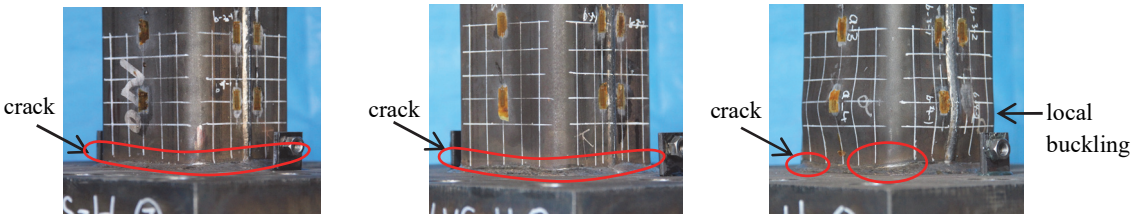

(a) LD12n30R25 (b) LD12n40R2 (c) LD12n40R25

Photo 1 –Test specimen after the experiment

3.2 Cyclic characteristics

Figure 7 shows the transition of the peak load which is defined by Q_i/Q_{max}, where, Q_i is a i-th cycle's lateral load at the maximum/minimum displacement and Q_{max} is a maximum strength. White and black circles indicate the positive side and negative side. The points when cracks and local buckling occurred are indicated by arrows. In the figure, F and W mean that local buckling occurred at the flange plate and the web plate, and added marks "+" and "-" mean the positive side and negative side respectively.

Strength of specimen with n=0.3 and R=2.5% gradually decreases and after the local buckling occurs at web side the strength drastically decreases further. By comparing the tendency of positive side with the negative side, it is observed that the strength of negative side decreases in a drastic manner after 27th cycles. Similarly, Strength of specimen with n=0.4 and R=2% gradually decreases and after cracks occurs followed by the local buckling at the web plate the strength of negative side drastically decreases. By comparing the tendency of positive side with the negative side, it is observed that the strength decreases in a drastic manner only in the negative side after crack occurred, however, the decrease becomes slowly again after 95th cycles. Strength of specimen with n=0.4 and R=2.5% gradually decreases and there is little difference between the positive side and the negative side.

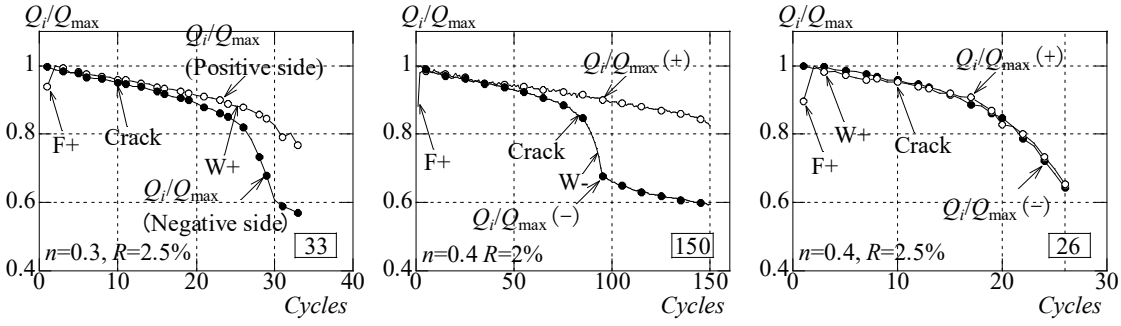

(a) LD12n30R25 (b) LD12n40R2 (c) LD12n40R25

Fig. 7 –Latelal load deterioration

According to Tables 8 and 9, local buckling at flange plates is firstly observed, then crack occurred and finally local buckling at web plates was observed in the specimens with n=0.3 and R=0.2% and n=0.4 and R=2.%. On the other hand, crack occurred after local buckling in the n=0.4 and R=2.5% specimen. Photo 2 shows the enlarged view of the test specimen's flange heat affected zone upper baseplate and cracks can be seen in red circles. Crack width of two specimens with slight deformation of local buckling (Photo-2 (a) and (b)) are relatively larger than that of the n=0.4 and R=2.5% specimen (Photo-2 (c)). It is assumed that failure modes are different and the modes affect the tendency of the strength deterioration.

Table 7 – Cycles when local buckling occurred

No.	Specimen	Flange	Web
1	LD12n30R25	1+	25+
2	LD12n40R2	1+	93-
3	LD12n40R25	1+	3+

Table 8 – Cycles when crack occurred

No.	Specimen	Cycle
1	LD12n30R25	10-
2	LD12n40R2	81-
3	LD12n40R25	10-

*Crack was observed at corner R at first

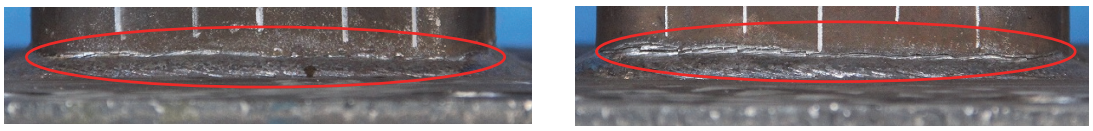

(a) n=0.3, R=2.5%

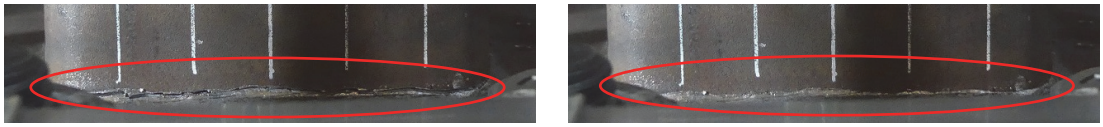

(b) n=0.4, R=2%

(c) n=0.4, R=2.5%

Photo 2 –Cracks at the heat affected zone upper the baseplate after the experiment

3.3 Limit-repeated cycle number

Table 9 shows the limit-repeated cycle number which is defined by the number of cycles that the lateral load at the maximum/minimum rotation angle decreased by 95%, 90%, 85% and 80% of the maximum lateral load. In Table 10, plasticity ratio μ ($=\theta/\theta_p$, θ=amplitude of rotation angle and θ_p is the plastic deformation which is the cross point of the plastic collapse mechanism line and elastic line) is shown. Test results obtained by the previous research are also shown in Table 10 Test specimens with similar test parameters

were selected, for example n= 0.3 and 0.4, l_k/D=10 and 14 and the steel tube was BCR295 (cold formed square steel pipe and F value is 295N/mm^2).

Figure 8 shows the relationship between the plasticity ratio μ and limit or repeated cycle number $N_{95\%}$ and $N_{80\%}$ with a logarithmic scale. According to these figures, the limit-repeated cycle numbers $N_{95\%}$ and $N_{80\%}$ have negative correlation with a plasticity ratio. By comparing with the results obtained by previous experimental study, it is observed that the relationship between $N_{95\%}$ and the plasticity ratio μ is almost same and the number of $N_{80\%}$ of this experimental study is smaller than the previous study. It is assumed that this is caused by the difference of the failure mode.

Table 9– Limit-repeated cycle number of this study

No.	Specimen	θ_p(%)	$\mu(\theta/\theta_p)$		$N_{95\%}$	$N_{90\%}$	$N_{85\%}$	$N_{80\%}$
1	LD12n30R25	1.61	1.55	+	12	22	28	30
				−	10	18	24	26
2	LD12n40R2	1.53	1.31	+	34	83	141	150+
				−	34	65	84	89
3	LD12n40R25	1.52	1.64	+	10	17	19	21
				−	10	16	19	21

Table 10– Limit-repeated cycle number of previous study

No.	Specimen	θ_p(%)	$\mu(\theta/\theta_p)$		$N_{95\%}$	$N_{90\%}$	$N_{85\%}$	$N_{80\%}$
1	LD10n30R15	0.67	2.24	+	4	6	11	18
				−	2	5	8	15
2	LD10n45R1	0.62	1.61	+	8	18	32	36
				−	9	19	31	36
3	LD14n30R15	0.92	1.63	+	8	15	26	44
				−	5	9	19	37
4	LD14n45R1	0.87	1.15	+	38	82	200+	-
				−	20	58	193	200+

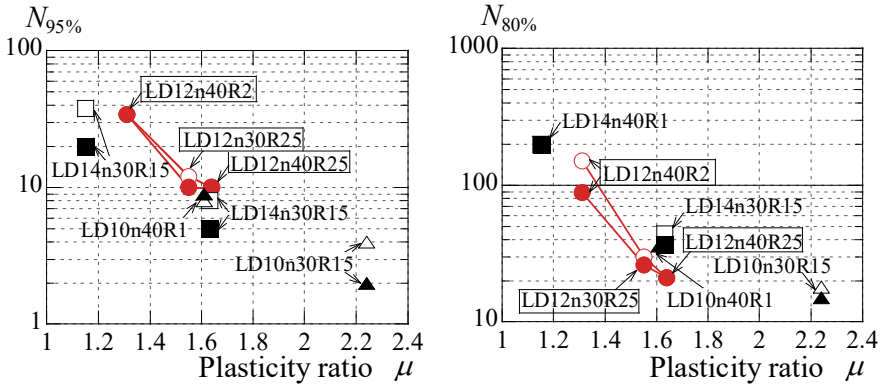

Fig. 8 –Limit-repeated cycle number and plasticity ratio relationship

4. Conclusions

From experimental results of three CFT beam-columns using H-SA700 steel subjected to constant axial compressive lad and cyclic horizontal load with constant amplitude of rotation angle, it has become clear that:

(1) Occurrence of cracks affects the strength deterioration in the specimen n=0.3 and R=2.5%, and in the specimen n=0.4 and R=2%. On the other hand, local buckling affects the strength deterioration in the specimen n=0.4 and R=2.5%. There are two failure modes which determine the strength deterioration behavior, the one is the crack dominant type and the other is the local buckling dominant type.

(2) A limit-repeated cycle number was defined. The relationship between the plasticity ratio and the limit-repeated cycle number $N_{95\%}$ and $N_{80\%}$ are shown and the limit-repeated cycle number has negative correlation with the plasticity ratio as same as the test results obtained by the experimental study of CFT beam-columns with BCR 295 steel tube.

Acknowledgements

This study was supported by the Grant-in-Aid for Scientific Research of Japan Society for the Promotion of Science. The authors would like to thank student in a structure and construction group in Kitakyushu University for their support of experimental work.

References

[1] Narihara, H. et al: Study on safety assessment methods for super-high-rise steel buildings against long-period earthquake ground motions, Part 27-31, *Summaries of Technical Paper of Annual Meeting*, Architectural Institute of Japan, C-III, pp.1251-1260, 2014.9 (in Japanese)

[2] Kido, M., Fukumoto, T., Tsuda, K., Ichinohe, Y. and Morita, K.: Study on the strength and cyclic rotation capacity of CFT beam-columns against long duration earthquake (report by committee), *Steel Construction Engineering*,pp.49-64 Vol. 24, No.94, 2017.6 (in Japanese)

[3] Kido, M., Tsuda, K., Fukumoto, T., Ichinohe, Y. and Morita, K.: Behavior of square concrete filled steel tubular beam- columns subjected to lateral load with constant cyclic displacement, *Journal of Structural and Construction Engineering (Transactions of AIJ)*, Vol.83, No.743, pp.725-735, 2019.5 (in Japanese)

[4] Utsunomiya, H., Kido, M. and Tsuda, K.: Study on influencing factors on the limit number of loading cycles of square CFT beam-columns, *AIJ Kyushu Chapter Architectural Research Meeting*, Vol.58, pp.40-408,2019.3 (in Japanese)

[5] Hayashi, K. et al: Restoring force characteristic and ultimate behavior of concrete filled steel tube columns using ultra-high strength steel H-SA700, *Journal of Structural and Construction Engineering (Transactions of AIJ)*, Vol.80, No.718, pp.2001-2009, 2015.12 (in Japanese)

[6] Hirata, H. et al: Flexural-shear behavior of ultra high strength concrete-filled steel tube column: *Proc. of Constructional Steel*, Vol.22, pp.577-582, 2014.11 (in Japanese)

[7] Hao, Y. and Kido, M.: Experimental study on a square CFT column with high strength steel tube: *Proc. of Constructional Steel*, Vol.23, pp. 792-797, 2015.11 (in Japanese)

